P2X7 signaling mediates migraine-related augmentation of meningeal afferent mechanosensitivity

Jun Zhao and Dan Levy*

Departments of Anesthesia, Critical Care and Pain Medicine, Beth Israel Deaconess Medical Center and Harvard Medical School, Boston, MA 02115

Number of text pages of the entire manuscript: 32; Number of Figures: 4; number of tables: 2

* **Correspondence:** Dr. Dan Levy, Department of Anesthesia, Critical Care, and Pain Medicine, 330 Brookline Avenue/DA 717, Boston, MA 02215. USA

Phone: 617-667-0534

E-mail: dlevy1@bidmc.harvard.edu

Abstract

Cortical spreading depolarization (CSD) is a key pathophysiological event that underlies visual and sensory auras in migraine. CSD further drives the headache phase in migraine by promoting the activation and sensitization of trigeminal meningeal sensory afferents. The factors responsible for this meningeal nociceptive response in the wake of CSD remain poorly understood, but potentially involve the local release of algesic, proinflammatory mediators, including ATP. Here, we used an in vivo extracellular single-unit recording of meningeal afferent activity in combination with topical administration of pharmacological agents in a rat model to explore the role of ATP-P2X receptor signaling in mediating CSD-evoked meningeal afferent activation and sensitization. We found that broad-spectrum inhibition of P2X receptors, P2X7 receptor antagonist, and blockade of the related pannexin1 channel suppressed CSD-evoked afferent mechanical sensitization, but did not affect afferent activation. Pharmacological inhibition of the pronociceptive P2X2,3 ATP receptor did not affect meningeal nociception post-CSD. Finally, we provide evidence supporting the notion that the anti-nociceptive effect mediated by P2X7 is localized to the meningeal and not the cerebral cortex. We propose that meningeal P2X7 and Panx1 signaling, potentially in meningeal macrophages or neutrophils mediates the mechanical sensitization of meningeal afferents, and contributes to migraine pain by exacerbating the headache during normally innocuous physical activities.

Keywords: Migraine, cortical spreading depolarization, meningeal afferents, mechanosensitivity, ATP, P2X7, pannexin 1.

1. Introduction

Migraine is a complex pain syndrome, one of the most common neurological disorders and the leading cause of disability in people under 50 [7; 36]. Migraine consists of episodic attacks characterized by a moderate-to-severe throbbing headache aggravated by physical activity and several other non-painful symptoms, including nausea and light sensitivity. The pathophysiological origin of migraine attacks remains poorly understood, although the headache phase is thought to involve output from trigeminal primary afferent neurons that innervate the cranial meninges [20]. Persistent discharge of meningeal afferents has been suggested to drive the ongoing migraine headache, and their augmented mechanosensitivity (i.e., sensitization) is thought to contribute to migraine pain by exacerbating the headache during normally innocuous physical activities that increase intracranial pressure and drive meningeal mechanical deformations [2; 12]. The factors underlying the triggering and maintenance of enhanced meningeal afferent responses in migraine remain incompletely understood. However, an acute meningeal inflammatory mechanism is considered to play a significant role [20].

Cortical spreading depolarization (CSD) is a key pathophysiological event that underlies visual and sensory auras in migraine, which often precede the headache phase [28]. CSD is a self-propagating slow wave of neuronal and glial depolarizations that drastically disrupts transmembrane gradients and cortical synaptic activity [29]. CSD triggering in rodent models produces prolonged activation and mechanical sensitization of meningeal nociceptive afferents [43; 47; 48] and can elicit pain behaviors reminiscent of the

headache pain of migraine [14; 16]. It is thus an important animal model that can be used to gain insights into the endogenous nociceptive processes that drive meningeal afferents in migraine. Animal studies have led to the theory that CSD is the primary driver of inflammatory nociceptive signaling and the ensuing headache in MA. In the wake of CSD, numerous algesic mediators are released into the cortical interstitium, including ATP, K^+, H^+, arachidonic acid, glutamate, and IL-1β. It has been proposed that these mediators reach the meninges via bulk diffusion or CSF flow, where they can act directly on meningeal afferents or influence their responses indirectly by promoting a meningeal inflammatory response [8; 11; 18; 27; 33; 38]. Cortical spreading depolarization (CSD) is a key pathophysiological event that underlies visual and sensory auras in migraine, which often precede the headache phase [28]. CSD is a self-propagating slow wave of neuronal and glial depolarizations that drastically disrupts transmembrane gradients and cortical synaptic activity [29]. CSD triggering in rodent models produces prolonged activation and mechanical sensitization of meningeal nociceptive afferents [43; 47; 48] and can elicit pain behaviors reminiscent of the headache pain of migraine [14; 16]. It is thus an important animal model that can be used to gain insights into the endogenous nociceptive processes that drive meningeal afferents in migraine. Animal studies have led to the theory that CSD is the primary driver of inflammatory nociceptive signaling and the ensuing headache in migraine with aura. In the wake of CSD, numerous algesic mediators are released into the cortical interstitium, including ATP, K^+, H^+, arachidonic acid, glutamate, and IL-1β. It has been proposed that these mediators reach the meninges via bulk diffusion or CSF flow, where they can act directly on meningeal

afferents or influence their responses indirectly by promoting a meningeal inflammatory response. [8; 11; 18; 27; 33; 38].

Here we focused on ATP signaling as a potential driver of meningeal nociception in the wake of CSD. ATP is a key algesic molecule that can act directly on nociceptive afferents by activating neuronal P2X2/3 receptors [5; 35]. ATP also serves as a danger-signaling molecule, part of the damage-associated molecular patterns released from stressed or damaged tissues [10], such as the cortex in the wake of CSD. ATP released in the context of tissue stress occurs partly via the opening of pannexin-1 (Panx1) channels [9] and CSD has been shown to stimulate the opening of Panx1 channels [16]. In the cortex, stimulation of P2X7 receptors by ATP controls CSD susceptibility [6]. However, diffusion of ATP across the cranial meninges and the stimulation of P2X7 expressed by meningeal immune cells [39] may also drive an inflammatory response and augment the responses of meningeal afferents [22; 31].

Here we tested the relative contribution of the ATP P2X receptors and panx1 signaling to the activation and sensitization of meningeal afferent in a rat model migraine with aura evoked by a single CSD. Using in vivo single-unit recording and a pharmacological approach we show that inhibition of the P2X7 receptor, and its related Panx1 channel, but not blockade of P2X2,3 channels suppress CSD-evoked meningeal afferent mechanical sensitization. We also demonstrate that P2X and Panx1 signaling do not mediate the CSD-evoked acute and persistent discharge of meningeal afferents. Finally, we provide evidence linking meningeal and not cortical P2X7 signaling to meningeal

afferent sensitization post-CSD.

2. Material and methods

2.1 *Animals*

All experiments were approved by the Institutional Animal Care and Use Committee of the Beth Israel Deaconess Medical Centre and followed the ARRIVE (Animal Research: Reporting of in vivo Experiments) guidelines [17]. Animals (Sprague-Dawley male rats, 220–250 g, Taconic, USA) were housed in pairs with food and water available *ad libitum* under a constant 12-hour light/dark cycle (lights on at 7:00 am) at room temperature. All procedures and testing were conducted during the light phase of the cycle (9:00 am to 4:00 pm). Experimental animals were randomly assigned to different treatment groups. No statistical methods were used to predetermine sample size for the experiments, but our sample sizes are similar to those reported in our previous publications using similar techniques [45; 48; 50].

2.2 *Surgical preparation for electrophysiological experiments*

Animals were deeply anesthetized with urethane (1.5 g/kg, i.p.) and mounted on a stereotaxic frame (Kopf Instruments). Core temperature was kept at 37.5–38°C using a homoeothermic control system. Animals were intubated and breathed O2-enriched room air spontaneously. Physiological parameters were collected throughout the experiments using PhysioSuite (Kent Scientific) and CapStar-100 (CWE). Data used in this report were obtained from animals exhibiting physiological levels of oxygen saturation (> 95%), heart

rate (350–450 beats/min), and end-tidal CO_2 (3.5–4.5%). Two separate craniotomies were made. One was used to expose the left transverse sinus and the posterior part of the superior sagittal sinus, including the adjacent cranial dura, extending ~2 mm rostral to the transverse sinus. Another small craniotomy (1 × 1 mm) was made over the right hemisphere. It was centered 2 mm caudal and 2 mm lateral to Bregma to allow insertion of the recording electrode into the trigeminal ganglion. A small burr hole (diameter, 0.5 mm) was drilled above the frontal cortex to induce CSD [49]. The exposed dura was bathed with a modified synthetic interstitial fluid (SIF) containing 135 mM NaCl, 5 mM KCl, 1 mM $MgCl_2$, 5 mM $CaCl_2$, 10 mM glucose, and 10 mM HEPES, pH 7.2.

2.3 *In vivo recording of meningeal afferent activity.*

Single-unit activity of meningeal afferents (1 afferent/rat) was recorded from their trigeminal ganglion somata using the contralateral approach reported earlier [50]. Meningeal afferents were identified by their constant response latency to electrical stimuli applied to the dura above the ipsilateral transverse sinus (0.5 ms pulse, 1-3 mA, 0.5 Hz). The response latency was used to calculate conduction velocity (CV) based on a conduction distance to the trigeminal ganglion of 12.5 mm [37]. Neurons were classified as Aδ ($1.5 \leq CV \leq 5$ m/s) or C afferents ($CV < 1.5$ m/s). Neural activity was digitized and sampled at 10 kHz using power 1401/Spike 2 interface (CED). A real-time waveform discriminator (Spike 2 software, CED) was used to create and store a template for the action potential evoked by electrical stimulation, which was used to acquire and analyze afferent activity.

2.4 Assessment of changes in meningeal afferent mechanosensitivity

Mechanical receptive fields (RF) of meningeal afferents were first identified as previously described using von Frey filaments [50]. To quantify changes in mechanical responsiveness, we used a servo force-controlled mechanical stimulator (Series 300B Dual Mode Servo System, Aurora Scientific). Mechanical stimuli were delivered using a flat-ended cylindrical plastic probe attached to the tip of the stimulator arm [50]. Two ramp-and-hold mechanical stimuli were applied in each trial (rise time, 100 msec; stimulus width, 2 sec; interstimulus interval, 120 sec) and included an initial threshold stimulus (which typically evoked at baseline 1–4 Hz responses) followed by a suprathreshold stimulus (2-3X of the threshold pressure). Stimulus trials were delivered every 15 min throughout the experiment to minimize response desensitization [50]. Ongoing activity was recorded continuously between the stimulation trials. Basal responses to mechanical stimuli were determined during at least four consecutive trials before the induction of CSD.

2.5 *Induction and monitoring of CSD*

A single CSD episode was induced in the left frontal cortex by briefly inserting a glass micropipette (50 µm diameter) ~2 mm deep into the cortex for 2 seconds [50]. Successful elicitation of CSD was evaluated by simultaneously recording changes in cerebral blood flow with a laser Doppler flowmetry probe positioned within the craniotomy, just above the exposed dura, ~1 mm from the RF of the recorded unit. The laser Doppler signal was digitized (100 Hz) and recorded using the power 1401/Spike 2. Baseline LDF data were based on recordings conducted for at least 30 min before CSD. Induction of CSD was

considered successful when the typical hemodynamic signature characterized by a large transient (~1 to 2 min) cortical hyperemia, followed by persistent (>1 hour) post-CSD oligemia, was observed **(Figure 1A)** [13].

2.6 Drugs and treatment approach

We used topical drug application to target local purinergic receptor signaling at the afferents' meningeal RF level. We used Pyridoxalphosphate-6-azophenyl-2',5'-disulfonic acid tetrasodium salt (PPDAS) as a non-selective P2X antagonist, and 2',3'-*O*-(2,4,6-Trinitrophenyl)adenosine-5'-triphosphate tetra(triethylammonium) salt (TNP-ATP) to inhibit $P2X_3$ and $P2X_{2,3}$ receptors. *N*-[2-[[2-[(2-Hydroxyethyl)amino]ethyl]amino]-5-quinolinyl]-2-tricyclo[3.3.1.13,7]dec-1-ylacetamide dihydrochloride (AZ 10606120) was used to inhibit P2X7, and (3β,20β)-3-(3-Carboxy-1-oxopropoxy)-11-oxoolean-12-en-29-oic acid disodium (carbenoxolone) was employed to inhibit Panx1. All pharmacological agents were purchased from Tocris and diluted in SIF for meningeal application. We first established the level of baseline ongoing activity and mechanosensitivity for 60 min in the presence of the vehicle (SIF). We then evaluated the change in the activity and mechanosensitivity of the afferents in the presence of the drugs for 60 min to ensure a lack of direct inhibitory effect on the afferents before CSD triggering. Post-CSD data was then collected in the presence of the drug or SIF (**Figure 1B**).

2.7 *Quantification and Statistical Analysis*

For analysis of afferent activity, N refers to the number of afferents. All data were analyzed and plotted using Prism 9 software and are presented as the median and interquartile

range (IQR). Group data in graphs show all data points and are plotted as scatter dot plots and the median. Statistical analyses are described in the results, figure legends, and below in this section. Differences in CSD-evoked afferent activation and sensitization propensities were analyzed using a two-tailed χ^2 test. All other data were analyzed using non-parametric two-tailed Mann Whitney or a Kruskal-Wallis tests followed by Dunn's post-hoc test. $p < 0.05$ was considered significant.

3. Results

ATP is a potent pronociceptive mediator that can drive activity in nociceptive afferents, including meningeal afferents [47]. CSD leads to cortical ATP efflux [25; 33]. Astrocytes are a key source of ATP [41], and blocking cortical astrocytic signaling inhibits the development of mechanical sensitization of meningeal afferents post-CSD [45]. Hence, we first examined the relative contribution of ATP signaling to this augmented afferent response post-CSD.

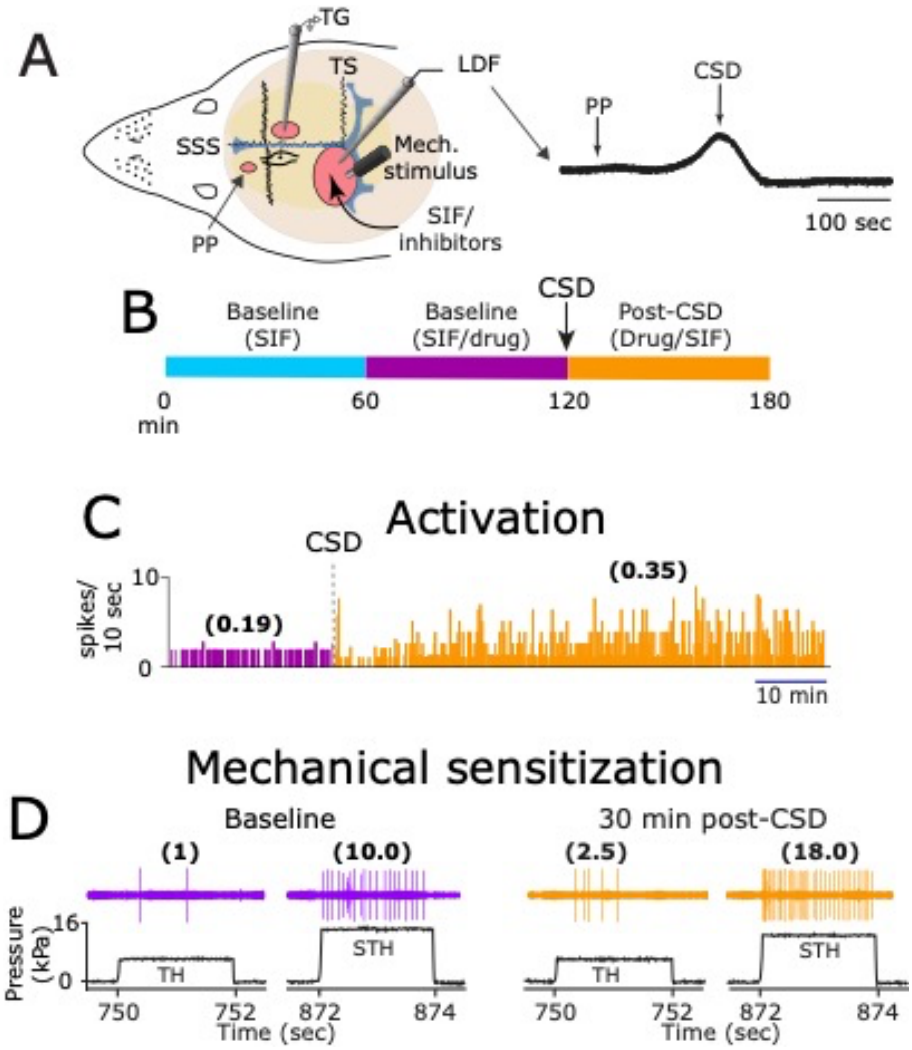

Figure 1. Experimental setup and testing paradigm. **A.** Experimental setup: three skull openings (red ovals) were made. A small burr hole was drilled over the left frontal cortex to elicit a single CSD event using a pinprick (PP) stimulation. Meningeal afferent activity was recorded in the left trigeminal ganglion (TG) using a tungsten microelectrode inserted through a craniotomy over the contralateral hemisphere. An ipsilateral craniotomy was made to expose a part of the left transverse sinus (TS) and superior sagittal sinus (SSS) and their vicinity to find and stimulate mechanosensitive meningeal afferents. Quantitative mechanical stimuli were delivered to the receptive field of afferents using a feedback-controlled mechanical stimulator. A Laser Doppler Flowmeter (LDF) probe was placed over the cortex near the receptive field of afferents to record changes in CBF and validate CSD induction noninvasively. Induction of CSD was considered successful when the typical hemodynamic signature characterized by a large transient (~1-2 min) cortical cerebral hyperemia (black trace), followed by persistent (>1 hour) post-CSD oligemia (blue trace) was observed. **B.** Experimental paradigm to test the effects of pharmacological blockers. **C.** Examples of an experiment depicting baseline ongoing activity (purple) and the acute and prolonged discharge of meningeal afferents post-CSD (orange) while the meninges are bathed with SIF. Afferent discharge rates in spikes/sec are in parentheses. **D.** Examples of experimental trials depicting the responses of a meningeal afferent to threshold (TH) and suprathreshold (STH) mechanical stimuli (black traces) during baseline recording and then at 30 min after CSD elicitation while the meninges are bathed with SIF. Responses in spikes/sec are in parentheses. Note the CSD-evoked TH and STH sensitization.

3.1 Broad-spectrum P2X antagonism suppresses CSD-evoked meningeal afferent mechanical sensitization

To examine the role of ATP signaling, we first tested the effect of local treatment with PPDAS (0.1mM). This broad-spectrum purinergic P2X receptor antagonist has been shown to block the nociceptive effects of ATP [30]. PPADS application did not affect CSD triggering (11/11 events), indicating no direct or indirect effects that could influence the vulnerability for CSD induction. We compared CSD-related changes in the mechanical responsiveness of 5 Aδ and 6 C afferents recorded from PPADS-treated animals with 9 Aδ and 13 C afferents recorded from vehicle-treated animals. The data obtained from the Aδ and C afferents were combined as they show similar sensitization characteristics after CSD [48]. While the afferents' baseline mechanosensitivity was not affected by PPADS ($p > 0.05$ vs. control for both TH and STH stimuli levels; **Table 1**), the post-CSD sensitization was markedly inhibited **(Figure 2)**. When mechanical sensitization was defined as enhanced responsiveness at either the TH or STH stimuli levels, we detected fewer sensitized afferents in the PPADS-treated group compared to the control group (2/11 vs. 17/23 sensitized afferents; $\chi^2 = 9.3$, $p<0.01$, **Figure 2B**]. PPADS treatment also inhibited afferent sensitization, defined as enhanced responsiveness at both TH and STH stimuli levels (PPADS: 0/11, Control: 10/23 sensitized afferents; $\chi^2=6.8$, $p<0.01$, **Figure 2C**). PPADS also decreased the overall changes in TH and STH responses post-CSD when compared to the vehicle [TH, -0.3 (1.6) spikes/sec vs. 0.9(1.7) spikes/sec, $p<0.05$; STH, 0.9(0.2) vs. 1.3 (0.7) fold, $p<0.001$, **Figures 2D, E**].

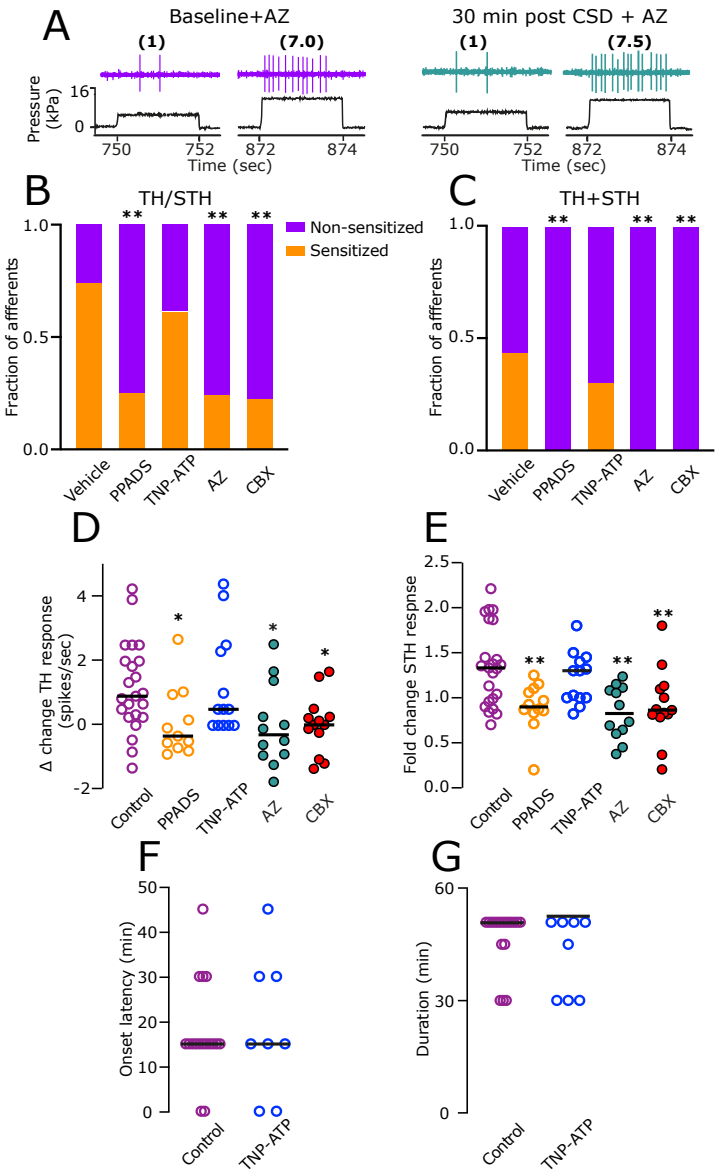

Figure 2. Inhibition of P2X7 receptors and Panx1 channels suppresses CSD-evoked mechanical sensitization of meningeal afferents. **A.** Examples of experimental trials depicting the responses of a meningeal afferent to threshold (TH) and suprathreshold (STH) mechanical stimuli during baseline recording and then at 30 min after CSD elicitation in the presence of the P2X7 receptor inhibitor AZ10606120 (AZ). Note the lack of sensitization at both the TH and STH stimuli levels. When compared to controls (n=22), the fraction of afferents that became sensitized at the TH or STH level (TH/STH, **B**) or at both levels (TH+STH, **C**) was lower in animals treated with the broad-spectrum purinergic P2X receptor antagonist PPADS (n=18), AZ10606120 (n=12), or the Panx1 inhibitor, carbenoxolone (CBX, n=13), $p < 0.05$, χ^2 test, treatment vs. control). Inhibition of P2X2/3 and P2X3 receptors with TNP-ATP (n=13) did not affect the sensitization response. At the population level, inhibition of P2X, P2X7, or Panx1 also decreased the magnitude of the TH **(D)** and STH **(E)** afferent responsiveness post-CSD. Significance p-values indicate Dunn's post hoc test between a given treatment and control following a significant ($p < 0.01$) Kruskal-Wallis test between all treatments. TNP-ATP treatment did not affect the afferents' TH and STH response magnitude post-CSD (**D, E**) ($p > 0.05$, Kruskal-Wallis). TNP-ATP also did not affect the onset latency **(F)** and duration of the post-CSD sensitization response (**G**) when compared to vehicle control, $p>0.05$ Mann Whitney test. Data in **D-G** include all data points. Lines represent the median.

3.2 P2X2/3 and P2X3 inhibition does not affect CSD-evoked meningeal afferent mechanical sensitization

We next tested the possibility that ATP produces meningeal afferent sensitization by acting upon P2X3 and P2X2/3, the principal P2X receptors expressed by meningeal and other primary afferent nociceptive neurons [5; 35]. We tested the effect of the potent P2X2/3 receptor antagonist TNP-ATP (0.1 mM), which has been shown to block ATP-mediated nociceptive neuron responses [4]. Topical application of TNP-ATP did not affect CSD triggering (13/13 events) and also did not affect the afferent sensitization response. Among the afferent tested (6Aδ; 7C), when sensitization was defined as enhanced responsiveness at either the TH or STH stimuli level, we observed sensitization in 8/13 afferent, not different than in controls (χ^2 = 0.6, p=0.44, **Figure 2B**). Similarly, TNP-ATP did not inhibit the CSD-evoked sensitization defined as enhanced responsiveness at both the TH and STH stimuli levels (3/13 sensitized afferents, χ^2 = 1.5, p>0.05, p=0.22, **Figure 2C**]. TNP-ATP treatment also resulted in similar sensitization magnitudes [TH, 0.5(2.4) spikes/sec, p>0.05 vs. control; STH, 1.3(0.4) fold, $p > 0.05$ vs. control; **Figure 2D, E**], latencies for developing sensitization [(15.0(26.5) min vs. (15 (7.5), p>0.05, and durations of the sensitized state [52.5(30.0) vs. 60(15) min, p> 0.05, **Figure 2F, G**].

3.3 P2X7 and Panx1 signaling mediate CSD-evoked meningeal afferent mechanical sensitization

P2X7 receptors are unique ATP receptors that mediate pro-inflammatory functions and are expressed in numerous meningeal immune cells [39]. Because a broad spectrum

P2X antagonism (PPADS), but not inhibition of $P2X_3$, $P2X_{2,3}$ (TNP-ATP) affected the CSD-evoked afferents' mechanosensitization, we next asked whether P2X7 might be involved. To test the contribution of this purinergic receptor we used the selective P2X7 receptor antagonist AZ10606120 (10 μm), which has been shown to block macrophage proinflammatory response [34]. We recorded CSD-evoked responses of 4Aδ and 8C afferents in animals treated topically with AZ10606120. We observed no effect on the elicitation of single CSD events (12/12 events) or changes in the afferents' baseline mechanosensitivity (**Table 1**). Administration of AZ10606120, however, significantly decreased the afferents' propensity to develop mechanical sensitization post-CSD, both when sensitization was defined as increases at TH or STH level (3/12 sensitized afferents, $\chi^2 = 7.7$, $p<0.01$ vs. control, **Figure 2B**) or at TH plus STH levels (0/12 sensitized afferents, $\chi^2 = 7.3$, $p < 0.01$ vs. control, **Figure 2C**). The post-CSD responses in animals pretreated with the P2X7 antagonist were also smaller when compared to vehicle-treated controls [TH, -0.3(2.9) spikes/sec, $p<0.01$ vs. control; STH, 0.8 (0.5) fold, $p<0.01$ vs. control, **Figure 2 D, E**].

P2X7 forms a complex with Panx1 channels that serve as a large pore channel and conduit for the further release of ATP plus other proinflammatory mediators, such as IL-1β [23]. Panx1 is co-expressed with P2X7 in several meningeal immune cells, including macrophages, dendritic cells, and T cells [39], pointing to its potential contribution to afferent sensitization post-CSD. Because P2X7 antagonists may also inhibit the P2X7/Panx1 pore activity and related ATP release [19; 40], we next tested the effect of

the Panx1 inhibitor carbenoxolone (CBX, 1mM) [24] on the responses of 7Aδ and 6 C afferents. Dural application of CBX did not affect CSD induction (13/13 events) or basal afferent mechanosensitivity (**Table 1**). Treatment with CBX, however, diminished the propensity of the afferents to develop mechanical sensitization, either at the TH or STH levels (3/13 sensitized afferents, χ^2=8.7, p<0.01 vs. control, **Figure 2B**) or at both TH and STH (0/13 sensitized afferents, χ^2 =7.8, p <0.01 vs. control, **Figure 2C**). The post-CSD changes in TH and STH responses in CBX-treated animals were also more minor when compared to controls (TH, 0.0(0.9) spikes/sec, p<0.01 vs. control; STH, 0.9 (0.3) fold, p<0.01 vs. control, **Figure 2D, E**).

3.4 CSD-evoked meningeal afferents' activation does not involve P2X receptor signaling or Panx1 activation

The mechanisms underlying meningeal afferent mechanical hyperresponsiveness following CSD appear independent of those responsible for the increased ongoing discharge [48; 50]. We, therefore, examined next whether P2X and Panx1 inhibition affects the CSD-evoked increases in the afferents' ongoing activity. We first analyzed the effect of the pharmacological inhibitors on the development of the acute afferent discharge that develops during or immediately after the passage of the CSD wave under the afferents' meningeal receptive field.

Topical application of PPDAS neither affected the afferents' baseline ongoing activity (**Table 2**) nor their acute activation in response to CSD. We observed acute activation in

2/5 Aδ and 2/6 C afferents, not different than in the vehicle control group (7/24 Aδ and 11/32 C; χ^2= 0.1, p >0.05 for the combined population, **Figure 3B**). Inhibition of P2X2/3 receptors was similarly ineffective. In the presence of TNP-ATP, baseline ongoing activity was not affected (**Table 2**) and the acute activation was similar to the control treatment (3/6 Aδ and 1/7 C afferents, χ^2 = 0.01 p > 0.05 vs. controls for the combined population, **Figure 3B**). Local application of the selective P2X7 receptor antagonist AZ10606120 also did not inhibit baseline ongoing activity (**Table 2**) or the acute activation (2/4 Aδ and 4/8 C-afferents, χ^2 = 1.4 p > 0.05 vs. controls). Similarly, Panx1 inhibition with CBX also did not inhibit the baseline ongoing activity (**Table 2**) or the acute response resulting in the activation of 4/7 Aδ and 3/6 C (χ^2 = 2.2 p > 0.05 vs. controls, **Figure 3B**). Overall, none of the inhibitors tested affected the magnitude of the acute activation (p > 0.05, Kruskal-Wallis test, **Figure 3C**).

We next examined whether inhibition of the purinergic receptors and pannexin 1 affects the development of prolonged afferent activation post-CSD. None of the inhibitors affected the prolonged increase in afferent discharge rate **(Figure 3D).** Following PPDAS treatment, we detected prolonged activation in 2/5 Aδ and 4/6 C afferents, not different from the activation observed in vehicle-treated animals (13/24 Aδ, 20/32 C; χ^2 = 2.1 p > 0.05 for the combined population). The propensity to develop prolonged activation post-CSD was also unaffected by TNP-ATP treatment (4/6 Aδ, 3/7 C; χ^2 = 0.001 p > 0.05 for the combined population vs. control). Treatment with AZ10606120 resulted in prolonged activation in 3/4 Aδ and 6/8 C-afferents. Also, not different from

the control group ($\chi^2 = 1.1$ $p > 0.05$ for the combined population). Finally, CBX application failed to inhibit the prolonged activation, which was observed in 5/6 Aδ and 5/7 C-afferents ($\chi^2 = 1.5$, $p > 0.05$ vs. controls for the combined population). While none of the drugs tested affected the magnitude or duration of the prolonged afferent activation ($p > 0.05$ for all comparisons, Kruskal-Wallis tests**, Figure 3E, F**), PPDAS, AZ10606120, and carbenoxolone shortened the onset latency ($p < 0.001$ Kruskal-Wallis test followed by post hoc tests **Figure 3G**), suggesting a potentiating effect.

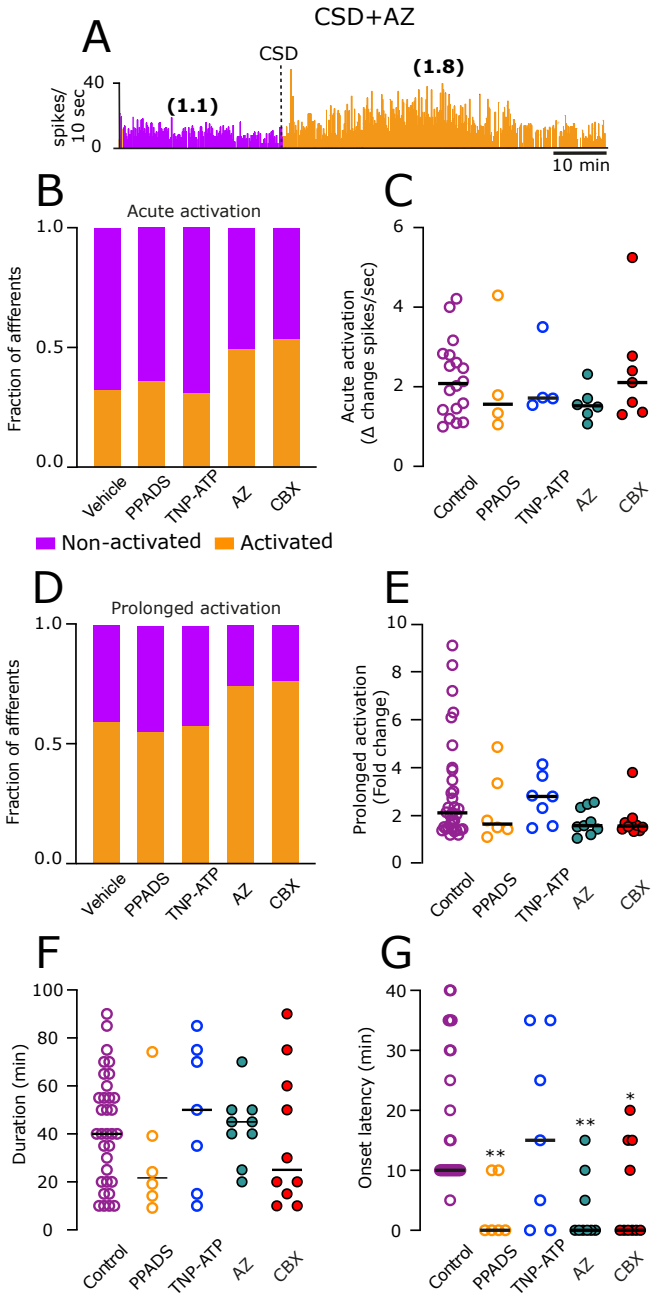

Figure 3. CSD-evoked meningeal afferent activation is not affected by pharmacological inhibition of P2X receptors and Panx1. **A**. Examples of experimental trials depicting the CSD-evoked acute and prolonged activation of a meningeal afferent in AZ10606120-treated animals. Ongoing activity (spikes/sec) is in parentheses. **B.** Broad spectrum P2X inhibition, selective antagonists of P2X2,3, P2X7, or Panx1 blockade did not affect the propensity of the afferents to develop acute activation ($p > 0.05$, χ^2 test for each treatment vs. control). **C.** The magnitude of the acute response was also not affected ($p > 0.05$ for all comparisons, Kruskal-Wallis test). **D.** Inhibition of P2X, P2X2,3, P2X7, or Panx1 also did not affect the propensity of the afferents to develop prolonged activation ($p > 0.05$, χ^2 test for each treatment vs. control). The magnitudes **(E)**, durations **(F),** and onset latencies **(G)** of the prolonged response were also not affected ($p > 0.05$ Kruskal-Wallis test for all comparisons vs. control). Data in **C, E-G** include all data points. Lines represent the median.

3.5 The meningeal anti-nociceptive effect mediated by P2X7 inhibition does not involve cortical action.

ATP diffused from the cortex can drive the activation of meningeal immune cells expressing P2X7 leading to afferent sensitization. However, activation of cortical astrocytic, microglial, and neuronal P2X7 receptors [15] might also play a role. Although we applied the pharmacological inhibitors topically to the meninges, it is technically challenging to ascertain whether they also diffused into the cortex. The cortical concentration of agents diffusing through the cranial meninges in this rat preparation is likely to be at least 1000-fold lower [46], which is expected to limit their cortical action. Nonetheless, we carried out an additional experiment to test whether AZ10606120 applied to the dura mater might also affect cortical P2X7-mediated responses.

Previous studies documented suppression of KCl-evoked CSD triggering in response to cortical P2X7/Panx1 pore activity inhibition [6], but not after Panx1 inhibition with carbenoxolone [16]. Building upon this previous data, we examined whether epidural application of AZ10606120 at the same concentration used to inhibit the meningeal afferent sensitization post-CSD suppresses multiple CSD triggering. We observed that AZ10606120 administration (n=4) did not affect the generation of multiple CSDs in response to continuous cortical KCl stimulation when compared to vehicle (n=4) treatment [AZ10606120 12.0 (3.5) CSDs/hr; vehicle 11.0 (4.2) CSDs/hr, $p>0.05$] suggesting that the effect of the topically applied AZ10606120 on the sensitization of meningeal was mediated via a meningeal action.

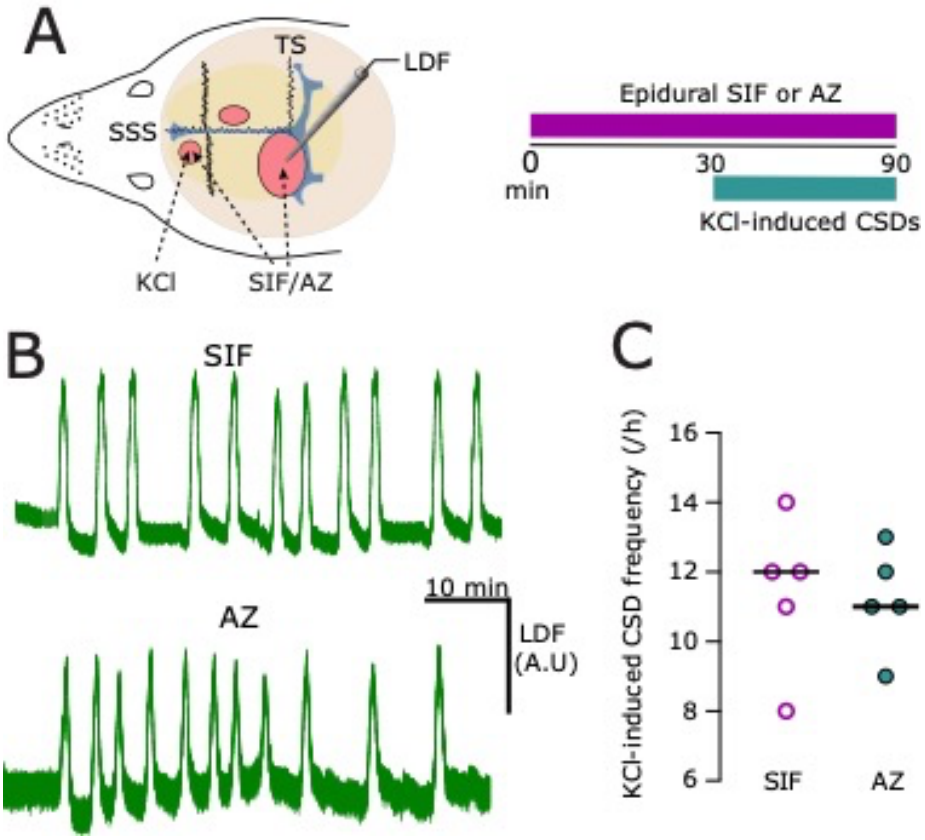

Figure 4. Epidural application of the P2X7 antagonist AZ10606120 (AZ) does not suppress the frequency of KCl-evoked cortical spreading depolarization (CSD). (**A**) Experimental setup and testing paradigm. **A.** We used the same surgical approach as in the TG recording, including three skull openings (red ovals). Continuous application of 1M KCl to the anterior burr hole was used to elicit multiple CSD events, monitored using laser doppler flowmetry (LDF) in the posterior opening. The burr hole and the site of LDF monitoring were pretreated with SIF or the P2X7 inhibitor (AZ10606120, 10 μm) for 30 min. CSD frequency was measured during the application of KCl in SIF or KCl+AZ. **B.** Representative LDF recordings show similar CSD frequencies in animals treated with SIF or AZ10606120. **C.** Scatter dot plot shows that P2X7 inhibition with AZ10606120 (n=4) does not inhibit KCl-evoked spreading depression frequency compared to vehicle (n=4). Data include all data points. Lines represent the median. $p>0.05$ Mann Whitney test.

4. Discussion

The headache phase in migraine with aura is thought to involve the activation and mechanical sensitization of meningeal afferents in response to a CSD event. However, the mechanisms by which CSD influences the responses of meningeal afferents have not been fully elucidated. Here we show that CSD augments the mechanosensitivity of meningeal afferents via the purinergic P2X7 channel and its related Panx1 pore. We further provide evidence supporting the notion that this meningeal anti-nociceptive effect is mediated by meningeal and not cortical P2X7-related signaling.

Our findings that blocking P2X7 and Panx1 interfere with the development of mechanical sensitization but does not impede the increase in afferent discharge post-CSD agrees with our previous data showing that the activation and sensitization of meningeal afferents, including in response to CSD, involves distinct mechanisms [45; 48; 50]. It should be noted that P2X7 and Panx1 inhibition, as well as the broad spectrum P2X inhibition, exerted some facilitatory effects on the prolonged increase in afferent discharge involving shortening the onset latency.

The mechanism by which P2X7/Panx1 activation drives meningeal afferent sensitization remains to be explored but likely involves an inflammatory response. Single-cell RNA sequencing data show the expression of P2X7 plus Panx1 in meningeal macrophages [39], pointing to macrophages as critical immune cells that mediate the afferent sensitization post-CSD. Activation of P2X7 and Panx1 signaling were also implicated in

meningeal neutrophil recruitment under pathological conditions [31] and thus could also play a role in mediating the meningeal nociceptive response produced by CSD. Meningeal P2X7/Panx1 activation can lead to the release of the pro-inflammatory and pronociceptive cytokines IL-1β and TNF- α plus the activation of phospholipase A2 and the release of sensitizing prostanoids [1; 21; 26]. IL-1β, TNF-α, and prostanoids have all been implicated in sensitizing meningeal afferents [42; 44; 50].

CSD gives rise to persistent vasodilatation of the middle meningeal artery, proposed to be mediated by prolonged activation of peptidergic meningeal afferents [3]. Karatas and colleagues [16] have shown that the local blockade of Panx1 with carbenoxolone suppresses this meningeal vasodilatory response. Our finding that carbenoxolone did not inhibit the CSD-evoked prolonged meningeal afferent activation argues however for a dissociation between the CSD-evoked dural vasodilatation enhanced ongoing meningeal afferent discharge. Whether signaling linked to the increased afferent mechanosensitivity post-CSD also exerts a local vasodilatory effect requires further investigation.

ATP is an algesic mediator that excites nociceptors, including meningeal afferents, by activating neuronal purinergic P2X2/3 receptors. Surprisingly, blocking this receptor using a potent antagonist failed to inhibit the increased afferent discharge post-CSD. Although activation of P2X2/3 by ATP may contribute to the afferent activation, the action of other algesic mediators that are co-released is likely more powerful in driving the discharge of meningeal afferents post-CSD.

Meningeal afferents are considered major players in migraine pain, yet our understanding of how they become engaged during a migraine attack is limited. We uncover a role for meningeal P2X7 signaling, involving also Panx1 megachannels in mediating the mechanical sensitization of meningeal afferents in a model of migraine of aura. Therapeutic approaches and clinical trials of P2X7 blockers are currently under development for various inflammatory conditions [32] and may be further explored for migraine treatment.

Conflict of Interest Statement:

The study was funded by NIH grants: R01NS086830, R01NS115972, R01NS078263, R21NS130561 to DL. The authors have no conflict of interest to declare.

Acknowledgment: Authors' contributions: J. Zhao and D. Levy performed experiments/data analyses; J. Zhao and D. Levy wrote and edited the manuscript; D. Levy conceived, designed, and led the project.

References:

[1] Barbera-Cremades M, Gomez AI, Baroja-Mazo A, Martinez-Alarcon L, Martinez CM, de Torre-Minguela C, Pelegrin P. P2X7 Receptor Induces Tumor Necrosis Factor-alpha Converting Enzyme Activation and Release to Boost TNF-alpha Production. Front Immunol 2017;8:862.

[2] Blaeser AS, Sugden AU, Zhao J, Carneiro-Nascimento S, Shipley FB, Carrie H, Andermann ML, Levy D. Trigeminal afferents sense locomotion-related meningeal deformations. Cell Rep 2022;41(7):111648.

[3] Bolay H, Reuter U, Dunn AK, Huang Z, Boas DA, Moskowitz MA. Intrinsic brain activity triggers trigeminal meningeal afferents in a migraine model. Nat Med 2002;8(2):136-142.
[4] Burgard EC, Niforatos W, van Biesen T, Lynch KJ, Touma E, Metzger RE, Kowaluk EA, Jarvis MF. P2X receptor-mediated ionic currents in dorsal root ganglion neurons. J Neurophysiol 1999;82(3):1590-1598.
[5] Burnstock G. Purinergic Mechanisms and Pain. Adv Pharmacol 2016;75:91-137.
[6] Chen SP, Qin T, Seidel JL, Zheng Y, Eikermann M, Ferrari MD, van den Maagdenberg A, Moskowitz MA, Ayata C, Eikermann-Haerter K. Inhibition of the P2X7-PANX1 complex suppresses spreading depolarization and neuroinflammation. Brain 2017;140(6):1643-1656.
[7] Collaborators GBDH. Global, regional, and national burden of migraine and tension-type headache, 1990-2016: a systematic analysis for the Global Burden of Disease Study 2016. Lancet Neurol 2018;17(11):954-976.
[8] Csiba L, Paschen W, Mies G. Regional changes in tissue pH and glucose content during cortical spreading depression in rat brain. Brain Res 1985;336(1):167-170.
[9] Dahl G, Qiu F, Wang J. The bizarre pharmacology of the ATP release channel pannexin1. Neuropharmacology 2013;75:583-593.
[10] Di Virgilio F, Sarti AC, Coutinho-Silva R. Purinergic signaling, DAMPs, and inflammation. Am J Physiol Cell Physiol 2020;318(5):C832-C835.
[11] Enger R, Tang W, Vindedal GF, Jensen V, Johannes Helm P, Sprengel R, Looger LL, Nagelhus EA. Dynamics of Ionic Shifts in Cortical Spreading Depression. Cerebral Cortex 2015;25(11):4469-4476.
[12] Gao YR, Drew PJ. Effects of Voluntary Locomotion and Calcitonin Gene-Related Peptide on the Dynamics of Single Dural Vessels in Awake Mice. J Neurosci 2016;36(8):2503-2516.
[13] Gariepy H, Zhao J, Levy D. Differential contribution of COX-1 and COX-2 derived prostanoids to cortical spreading depression-Evoked cerebral oligemia. J Cereb Blood Flow Metab 2017;37(3):1060-1068.
[14] Harriott AM, Chung DY, Uner A, Bozdayi RO, Morais A, Takizawa T, Qin T, Ayata C. Optogenetic spreading depression elicits trigeminal pain and anxiety behavior. Annals of Neurology 2020.
[15] Illes P, Khan TM, Rubini P. Neuronal P2X7 Receptors Revisited: Do They Really Exist? J Neurosci 2017;37(30):7049-7062.
[16] Karatas H, Erdener SE, Gursoy-Ozdemir Y, Lule S, Eren-Kocak E, Sen ZD, Dalkara T. Spreading Depression Triggers Headache by Activating Neuronal Panx1 Channels. Science 2013;339(6123):1092-1095.
[17] Kilkenny C, Browne WJ, Cuthi I, Emerson M, Altman DG. Improving bioscience research reporting: the ARRIVE guidelines for reporting animal research. Vet Clin Pathol 2012;41(1):27-31.
[18] Lauritzen M, Hansen AJ, Kronborg D, Wieloch T. Cortical spreading depression is associated with arachidonic acid accumulation and preservation of energy charge. J Cereb Blood Flow Metab 1990;10(1):115-122.

[19] Leeson HC, Kasherman MA, Chan-Ling T, Lovelace MD, Brownlie JC, Toppinen KM, Gu BJ, Weible MW, 2nd. P2X7 Receptors Regulate Phagocytosis and Proliferation in Adult Hippocampal and SVZ Neural Progenitor Cells: Implications for Inflammation in Neurogenesis. Stem Cells 2018;36(11):1764-1777.
[20] Levy D, Labastida-Ramirez A, MaassenVanDenBrink A. Current understanding of meningeal and cerebral vascular function underlying migraine headache. Cephalalgia 2019;39(13):1606-1622.
[21] Mariathasan S, Weiss DS, Newton K, McBride J, O'Rourke K, Roose-Girma M, Lee WP, Weinrauch Y, Monack DM, Dixit VM. Cryopyrin activates the inflammasome in response to toxins and ATP. Nature 2006;440(7081):228-232.
[22] McDonald B, Pittman K, Menezes GB, Hirota SA, Slaba I, Waterhouse CC, Beck PL, Muruve DA, Kubes P. Intravascular danger signals guide neutrophils to sites of sterile inflammation. Science 2010;330(6002):362-366.
[23] Mehta VB, Hart J, Wewers MD. ATP-stimulated release of interleukin (IL)-1beta and IL-18 requires priming by lipopolysaccharide and is independent of caspase-1 cleavage. J Biol Chem 2001;276(6):3820-3826.
[24] Michalski K, Kawate T. Carbenoxolone inhibits Pannexin1 channels through interactions in the first extracellular loop. J Gen Physiol 2016;147(2):165-174.
[25] Mies G, Paschen W. Regional changes of blood flow, glucose, and ATP content determined on brain sections during a single passage of spreading depression in rat brain cortex. Exp Neurol 1984;84(2):249-258.
[26] Norris PC, Gosselin D, Reichart D, Glass CK, Dennis EA. Phospholipase A2 regulates eicosanoid class switching during inflammasome activation. Proc Natl Acad Sci U S A 2014;111(35):12746-12751.
[27] Parker PD, Suryavanshi P, Melone M, Sawant-Pokam PA, Reinhart KM, Kaufmann D, Theriot JJ, Pugliese A, Conti F, Shuttleworth CW, Pietrobon D, Brennan KC. Non-canonical glutamate signaling in a genetic model of migraine with aura. Neuron 2021;109(4):611-628 e618.
[28] Pietrobon D, Moskowitz MA. Pathophysiology of migraine. Annu Rev Physiol 2013;75:365-391.
[29] Pietrobon D, Moskowitz MA. Chaos and commotion in the wake of cortical spreading depression and spreading depolarizations. Nat Rev Neurosci 2014;15(6):379-393.
[30] Rong W, Burnstock G. Activation of ureter nociceptors by exogenous and endogenous ATP in guinea pig. Neuropharmacology 2004;47(7):1093-1101.
[31] Roth TL, Nayak D, Atanasijevic T, Koretsky AP, Latour LL, McGavern DB. Transcranial amelioration of inflammation and cell death after brain injury. Nature 2014;505(7482):223-228.
[32] Rotondo JC, Mazziotta C, Lanzillotti C, Stefani C, Badiale G, Campione G, Martini F, Tognon M. The Role of Purinergic P2X7 Receptor in Inflammation and Cancer: Novel Molecular Insights and Clinical Applications. Cancers (Basel) 2022;14(5).
[33] Schock SC, Munyao N, Yakubchyk Y, Sabourin LA, Hakim AM, Ventureyra EC, Thompson CS. Cortical spreading depression releases ATP into the extracellular

space and purinergic receptor activation contributes to the induction of ischemic tolerance. Brain Res 2007;1168:129-138.
[34] Sluyter R, Vine KL. N-Alkyl-Substituted Isatins Enhance P2X7 Receptor-Induced Interleukin-1beta Release from Murine Macrophages. Mediators of inflammation 2016;2016:2097219.
[35] Staikopoulos V, Sessle BJ, Furness JB, Jennings EA. Localization of P2X2 and P2X3 receptors in rat trigeminal ganglion neurons. Neuroscience 2007;144(1):208-216.
[36] Steiner TJ, Stovner LJ, Vos T, Jensen R, Katsarava Z. Migraine is first cause of disability in under 50s: will health politicians now take notice? J Headache Pain 2018;19(1):17.
[37] Strassman AM, Raymond SA, Burstein R. Sensitization of meningeal sensory neurons and the origin of headaches. Nature 1996;384(6609):560-564.
[38] Takizawa T, Shibata M, Kayama Y, Toriumi H, Ebine T, Koh A, Shimizu T, Suzuki N. Temporal profiles of high-mobility group box 1 expression levels after cortical spreading depression in mice. Cephalalgia 2016;36(1):44-52.
[39] Van Hove H, Martens L, Scheyltjens I, De Vlaminck K, Pombo Antunes AR, De Prijck S, Vandamme N, De Schepper S, Van Isterdael G, Scott CL, Aerts J, Berx G, Boeckxstaens GE, Vandenbroucke RE, Vereecke L, Moechars D, Guilliams M, Van Ginderachter JA, Saeys Y, Movahedi K. A single-cell atlas of mouse brain macrophages reveals unique transcriptional identities shaped by ontogeny and tissue environment. Nat Neurosci 2019;22(6):1021-1035.
[40] Xia J, Lim JC, Lu W, Beckel JM, Macarak EJ, Laties AM, Mitchell CH. Neurons respond directly to mechanical deformation with pannexin-mediated ATP release and autostimulation of P2X7 receptors. J Physiol 2012;590(10):2285-2304.
[41] Xiong Y, Sun S, Teng S, Jin M, Zhou Z. Ca(2+)-Dependent and Ca(2+)-Independent ATP Release in Astrocytes. Front Mol Neurosci 2018;11:224.
[42] Zhang X, Burstein R, Levy D. Local action of the proinflammatory cytokines IL-1beta and IL-6 on intracranial meningeal nociceptors. Cephalalgia 2012;32(1):66-72.
[43] Zhang X, Levy D, Noseda R, Kainz V, Jakubowski M, Burstein R. Activation of meningeal nociceptors by cortical spreading depression: implications for migraine with aura. J Neurosci 2010;30(26):8807-8814.
[44] Zhang XC, Kainz V, Burstein R, Levy D. Tumor necrosis factor-alpha induces sensitization of meningeal nociceptors mediated via local COX and p38 MAP kinase actions. Pain 2011;152(1):140-149.
[45] Zhao J, Blaeser AS, Levy D. Astrocytes mediate migraine-related intracranial meningeal mechanical hypersensitivity. Pain 2021;162(9):2386-2396.
[46] Zhao J, Bree D, Harrington MG, Strassman AM, Levy D. Cranial dural permeability of inflammatory nociceptive mediators: Potential implications for animal models of migraine. Cephalalgia 2017;37(11):1017-1025.
[47] Zhao J, Levy D. Modulation of intracranial meningeal nociceptor activity by cortical spreading depression: a reassessment. J Neurophysiol 2015;113(7):2778-2785.

[48] Zhao J, Levy D. Cortical Spreading Depression Promotes Persistent Mechanical Sensitization of Intracranial Meningeal Afferents: Implications for the Intracranial Mechanosensitivity of Migraine. eNeuro 2016;3(6):ENEURO.0287-0216.2016.
[49] Zhao J, Levy D. The CGRP receptor antagonist BIBN4096 inhibits prolonged meningeal afferent activation evoked by brief local K(+) stimulation but not cortical spreading depression-induced afferent sensitization. Pain Rep 2018;3(1):e632.
[50] Zhao J, Levy D. Dissociation between CSD-Evoked Metabolic Perturbations and Meningeal Afferent Activation and Sensitization: Implications for Mechanisms of Migraine Headache Onset. J Neurosci 2018;38(22):5053-5066.

Table 1: Baseline mechanical response properties of meningeal afferents in animals treated with vehicle (control), PPADS, TNP-ATP, AZ10606120 (AZ), Carbenoxolone (CBX)

	Meningeal mechanical RFs	TH responses	STH responses
Vehicle (n=23)	2(1)	1.5(2.2)	8.0(6.5)
PPADS (n=11)	2(2)	1.8 (1.8)	7.8(5.6)
TNP-ATP (n=13)	2(1)	2.0(1.4)	7.3(11.0)
AZ (n=12)	2(1)	2.5(1.5)	7.0(6.1)
CBX (n=12)	2(2)	2.0(1.6)	8.3(10.6)

Data are expressed as median (IQR). N represents the number of afferents tested (1 afferent/animal). The number of distinct dural receptive fields (RFs) was tested using a suprathreshold von Frey stimulus. Threshold (TH) and suprathreshold (STH) responses (in spikes/second) are based on activity recorded during a 2-s stimulation and represent the average of 4 trials conducted before CSD while the afferent RF was bathed with vehicle or drug. Group differences were analyzed using the 2-tailed Kruskal–Wallis test and were not significant ($P > 0.05$) for the 3 parameters tested.

Table 2: Baseline ongoing activity in animals treated with vehicle, PPADS, TNP-ATP, AZ10606120 (AZ), or Carbenoxolone (CBX)

	Aδ	**C**	**Combined population**
Vehicle	(n=23); 0.1(0.2)	(n=33); 0.6(1.4)	0.2(.8)
PPADS	(n=5); 0.05 (0.7)	(n=6); 1.2(1.6)	0.4 (1.2)
TNP-ATP	(n=6); 0.1(0.2)	(n=7); 0.7(1.7)	0.1(1)
AZ	(n=4); 0.1 (0.2)	(n=8); 0.6(1.2)	0.3(0.8)
CBX	(n=7); 0.2 (0.5)	(n=8); 1.3(2)	0.4 (1.5)

Data are expressed as median (IQR). N represent the number of afferents tested (1 afferent/animal). Ongoing activity (in spikes/sec) is based on data collected for at least 45 minutes before CSD while the RF of the afferents was bathed with the drug or vehicle (SIF). Group differences were analyzed using 2-tailed Kruskal–Wallis test and were not significant ($P > 0.05$) for the population tested.